International Journal for Housing Science and Its Applications
Publish August 4, 2025. Volume 46, Issue 3 Pages 1344-1356

https://doi.org/10.70517/ijhsa463104

Assessment of photovoltaic carrying capacity and uncertainty analysis of county distribution networks based on stochastic differential equation modeling

Jian Zhao[1], Ning Zhou[1,*], Ling Miao[1], Jianwei Ma[1], Hao Liu[1], Yurong Hu[1] and Yuping Wei[2]
[1] Electric Power Research Institute, State Grid Henan Electric Power Company, Zhengzhou, Henan, 450052, China
[2] Sichuan Energy Internet Research Institute, Tsinghua University, Chengdu, Sichuan, 610213, China
Corresponding authors: (e-mail: zhouningznzn@163.com).

Abstract The article constructs the covariance matrix as well as the mean vector of the stochastic differential equation and tests its hypotheses using the EM algorithm estimation. The model is applied to the PV carrying capacity assessment of county distribution networks, and the method is utilized to solve for the maximum PV capacity under the constraints such as the discard rate. Meanwhile, the distribution of PV carrying capacity prediction error uncertainty is analyzed by cloud modeling, and the kernel density estimation is used to quantify the prediction error confidence interval. Combined with the collected PV historical operation and real-time observation data, the carrying capacity assessment and uncertainty analysis are carried out. When the PV abandonment rate is 3.5%, the maximum overload and maximum network loss are 6.495 MW and 0.712 MW, respectively, and the PV acceptable capacity reaches a steady state. The results of PV carrying capacity assessment of this paper's method and Monte Carlo method in power supply station area are close to 6.73MW and 6.71MW, respectively, but the calculation time of this paper's method is faster. The application of stochastic differential equation modeling yields high accuracy of PV carrying capacity prediction results, which fall completely inside the 85% to 95% confidence interval. The PV carrying capacity prediction result of this paper's method for 816 households in a county is 2652 kW. This paper's method can effectively predict the PV carrying capacity of county distribution networks and realize accurate assessment. The confidence interval of the carrying capacity is quantified by combining the nonparametric kernel density estimation method.

Index Terms stochastic differential equation, nonparametric kernel density, carrying capacity assessment, uncertainty analysis

I. Introduction

With the continuous development of China's economy and the continuous improvement of urban and rural power grid construction, county distribution grid projects occupy a very important position in China's power industry [1], [2]. County distribution grid project refers to the engineering project to renovate and upgrade the distribution grid within the county to improve the reliability of power supply, reduce the line loss rate, improve the quality of power supply, and improve the efficiency of power grid operation [3]-[6]. In order to ensure the effective implementation of the project and the continuous improvement of the project results, it is particularly important to assess and analyze the PV carrying capacity and uncertainty of the county distribution grid projects [7]-[9].

With the rapid development of distributed PV, its high percentage of large-scale access has become the future development trend of distribution grid [10], [11]. However, due to the random volatility of PV power generation, it makes the problems of voltage overrun and current backflow more serious during distribution network operation [12]. In order to guarantee the safe and coordinated development of distribution network source-network-load, it is important to assess the distributed PV carrying capacity to guide the distributed PV scale access based on the stable operation boundary of the distribution network and the actual operation state [13]-[15]. The PV carrying capacity assessment needs to be carried out from the technical, environmental, socio-economic and other dimensions to ensure the scientific and sustainability of the whole life cycle of the project [16], [17]. The assessment process is divided into six core aspects: site selection, resource calculation, equipment selection, system design, environmental impact prediction, and social benefit analysis, each of which requires the establishment of a quantitative index system and a dynamic monitoring mechanism [18]-[20]. As the PV carrying capacity is largely susceptible to environmental, meteorological and other uncertainties, the volatility of its output under high penetration scenarios has brought a series of adverse effects on the operational security of the distribution network [21]-[23]. Therefore, it is of practical significance to analyze the uncertainty of PV carrying capacity, quantify the

operational risk level of the distribution network, and take reasonable measures to control the risk, in order to improve the security of the distribution network operation and ensure the quality of power supply to users [24]-[26].

In this paper, we propose a stochastic differential equation model-based PV carrying capacity assessment method for distribution grids to quantify the impact of PV processing uncertainty on the carrying capacity of distribution grids. By inputting the PV capacity of the distribution grid and generating stochastic operation scenarios, the PV abandonment rate under different scenarios is calculated. The model is utilized to solve for the maximum PV capacity using the operating states of different PV operating scenarios and the discard rate as constraints. The probability distribution and cumulative distribution of random samples are calculated to quantitatively analyze the PV carrying capacity prediction error uncertainty. By mining county distribution network data, PV equipment rating data, and operation data, the corresponding data are selected for distribution network PV carrying capacity assessment.

II. Methodology

II. A. One-dimensional stochastic differential equation modeling

In this study, one-dimensional stochastic differential equations are constructed within the framework of distribution network system, and appropriate covariance matrices are established for the characteristics of the grid, and various covariance matrices [27], such as AR(1), SAD(1), and Brownian process, are added to accommodate the differences in the phenotypes, so as to construct a complete stochastic framework.

II. A. 1) Construction of the covariance matrix

Extending the dependence model to fit the structure of the time-dependent variance and correlation results in a structured dependence (SAD) model. In this study, SAD is used as a covariance model, consisting of the correlated variance $_{v}$ and the structure of the correlation φ as follows:

$$\sigma^2(t)=\frac{1-\varphi^{2t}}{1-\varphi^2}v^2,\quad t=1,\ldots,T \tag{1}$$

When $t_2>t_1$, the correlation coefficient function of the SAD model can be written in the following form:

$$corr(\sigma(t_1),\sigma(t_2))=\varphi^{t_2-t_1},t_2>t_1 \tag{2}$$

The following form is obtained:

$$\sum=v^2\begin{pmatrix} 1 & \varphi & \varphi^2 & \cdots & \varphi^{T-1} \\ \varphi & \frac{1-\varphi^4}{1-\varphi^2} & \varphi\frac{1-\varphi^4}{1-\varphi^2} & \cdots & \varphi^{T-2} \\ \vdots & \vdots & \vdots & \ddots & \vdots \\ \varphi^{T-2} & \varphi^{T-3}\frac{1-\varphi^4}{1-\varphi^2} & \varphi^{T-4}\frac{1-\varphi^6}{1-\varphi^2} & \cdots & \varphi\frac{1-\varphi^{2(T-1)}}{1-\varphi^2} \\ \varphi^{T-1} & \varphi^{T-2}\frac{1-\varphi^4}{1-\varphi^2} & \varphi^{T-3}\frac{1-\varphi^6}{1-\varphi^2} & \cdots & \frac{1-\varphi^{2T}}{1-\varphi^2} \end{pmatrix} \tag{3}$$

The correlation function of the SAD model is non-smooth because the correlation depends not only on the time interval t_2-t_1 but also on the correlation structure φ. Therefore, the covariance matrix can be simplified by parameterizing (φ,v).

II. A. 2) Mean Vector Modeling

Considering that the distribution system often encounters the influence of environmental factors, it is of wide interest to study whether fluctuations affect the biological system and whether they cause a change in the already existing results, where the effect of environmental fluctuations on the PV carrying capacity is investigated by introducing a perturbation term, so that the equation can be expressed as follows:

$$dx(t)=rx(t)(1-\frac{x(t)}{K})dt+\sigma_w dw_t \tag{4}$$

A quantitative measure of model uncertainty can be obtained if the parameters of the diffusion term are estimated simultaneously. Since equation (4) a nonlinear stochastic differential equation under its Ito integral form:

$$x(t) = x(t_0) + r\int_0^t x(s)(1-\frac{x(s)}{K})ds + \sigma_w w_t \tag{5}$$

where $x(t_0)$ is a random variable independent of the Wiener process and it can only be a constant.

It is clear that σ_w in the equation is independent of x_t, so the results are the same using Stratonovich integration [28] and Ito integration [29]. This is because the drift term of the equation is nonlinear and the diffusion term is a constant, so it is not possible to integrate to obtain a solution to the equation.

In the study only the first and second order moments of the solution are required and these moments can be obtained in a simple way. The specific solution is also given next.

The KEF is used to obtain the mean of the multivariate normal distribution, which is the same as predicted below:

$$\hat{y}_{k|k-1} = E(y_k \mid Y_{k-1}, \Omega) \tag{6}$$

The same conditional density prediction variance is:

$$R_{k|k-1} = V(y_k \mid Y_{k-1}, \Omega) \tag{7}$$

The above representation is also used for the mean and variance of the first prediction, and the initial condition of the EKF is $\hat{y}_{1|0} = E(y_{t_0}), R_{1|0}$, which is the mean and variance of the initial state of equation (4). The predicted mean $\mu_j = c(u_j(1),\ldots,\mu_j(T))$ is obtained according to equations (6) and (7). Thereby, according to equation (4) can be reduced to the parameters (σ_w, r, K).

II. A. 3) Hypothesis testing

The parameters of this mean and covariance structure established can be estimated using the EM algorithm. Optimization of the likelihood function provides estimates of the parameter covariances given by the negative inverse Hessian of the log-likelihood evaluated at the best parameter value. Thus, the existence of a significant QTL can be tested by the following hypothesis test:

$$\mathrm{H0}: (r_j, K_j, \sigma_{wj}) = (r, K, \sigma_w) \quad for \quad j = 1,\cdots,J \tag{8}$$

$$\mathrm{H1}: \text{ At least one of the above equations is not true} \tag{9}$$

where H0 corresponds to the simplified model of PV carrying capacity without the influence of factors and H1 corresponds to the full model with the presence of factors, as well as this log-likelihood values L0 and L1 are obtained by calculating under H0 and HI. Then, the likelihood ratios of these two types of assumptions are calculated:

$$LR = -2\ln(\frac{L_0}{L_1}) \tag{10}$$

The log-likelihood ratio (LR) of the obtained full model was calculated and compared with the critical threshold.

II. B. Carrying capacity assessment model of distribution network based on light abandonment rate

II. B. 1) Basic principles

Based on the basic principle of distributed PV systems, PV inverters have the function of regulating abandoned light. When the grid voltage exceeds the limit, the PV inverter can reduce the active and reactive power injected into the grid by the PV system by adjusting the output power, so as to effectively regulate the voltage that exceeds the limit to within the normal range. This regulation process can respond to the changes in the grid operation state in real time to maintain the stable operation of the grid.

In this paper, the statistical value of the abandoned light rate under various operating scenarios after distributed PV access does not exceed a given limit value as a constraint, and the distributed PV access capacity that satisfies the abandoned light rate constraint is determined based on the opportunity constraint. Different levels of light abandonment rate correspond to different carrying capacities, and the higher the allowable light abandonment rate means the stronger the ability to regulate the operation indexes exceeding the limit by regulating the light abandonment, so the carrying capacity of distributed PV access to the distribution grid can be improved.

II. B. 2) Objective function

In this paper, we study the assessment of the carrying capacity of distributed photovoltaic (PV) access to the distribution network, and set the maximum capacity of distributed PV accessed by the distribution network as the objective function:

$$\max F_1 = \max \sum_{i=1}^{n} P_{DG.i} \tag{11}$$

where P_{DG} is the i th distributed PV capacity and n is the number of distributed PVs connected to the distribution grid.

II. B. 3) Constraints

(1) Operational state constraints:

a) Currents Balance:

$$\begin{cases} P_{DG,i} - P_i - U_i \sum_{j=1}^{n} U_j (G_{ij} \cos\theta_{ij} + B_{ij} \sin\theta_{ij}) = 0 \\ Q_{DG,i} - Q_i - U_i \sum_{j=1}^{n} U_j (G_{ij} \sin\theta_{ij} - B_{ij} \cos\theta_{ij}) = 0 \end{cases} \tag{12}$$

where $P_{DG,i}, Q_{DG,i}$ is the active and reactive output of the distributed PV at the i th node. P_i, Q_i is the active and reactive load of the i th node. G_{ij}, B_{ij} is the conductance, conductor distributed on the wire from the i th node to the j th node. θ_{ij} is the phase angle difference at nodes i, j.

b) Voltage crossing:

$$U_{\min} < U_n < U_{\max} \tag{13}$$

where $U_{\max}$ and $U_{\min}$ are the upper and lower limits of the line voltage, respectively.

c) Current constraints:

$$0 \le I_i \le I_{\max} \tag{14}$$

where I_i is the current flowing on branch i and $I_{\max}$ is the maximum current allowed to flow on the branch.

d) Branch transmission capacity constraint:

$$0 \le S_i \le S_{\max} \tag{15}$$

where S_i is the actual transmission capacity of line i and $S_{\max}$ is the rated transmission capacity of the line. If the transmission capacity of a branch line exceeds its design or carrying capacity, it may lead to overloading of equipment, accelerating equipment aging or even damage, thus affecting the reliability and stability of the power grid.

(2) Light abandonment rate constraint:

$$\eta = \frac{P_{q,i}}{P_{DG,i}} \tag{16}$$

where $P_{q,i}$ is the amount of distributed PV abandoned at the i th node and $P_{DG,i}$ is the actual output of distributed PV at the i th node. And:

$$\eta \le \eta_{\max} \tag{17}$$

where η is the actual abandonment rate and $\eta_{\max}$ is the maximum abandonment rate.

II. B. 4) Model solving

Based on the opportunity constraint for distributed PV carrying capacity model, the solution steps are as follows:

(1) Input distribution network system parameters and distributed PV capacity. Including topology and line parameters, as well as the load of each node and the set distributed PV capacity.

(2) Generate stochastic scenarios. A stochastic differential equation method is used to extract a large number of stochastic PV output curves from the output model.

(3) Calculate the amount of abandoned light. For each random PV output curve sampled based on the stochastic differential equation method, it is compared with the safety constraints. If the PV output exceeds the constraint, the amount of light discarded for that curve is calculated.

(4) Calculate the light abandonment rate. Sum the discarded light from all random PV output curves and divide by the total PV generation to get the final discard rate.

(5) Repeat (3) and (4) as the installed capacity of distributed PV increases gradually until the light abandonment rate reaches the preset constraints. At this point, the access capacity of distributed PV is the maximum access capacity.

II. C. Uncertainty analysis of wind power prediction error

II. C. 1) Fundamentals

In this section, cloud modeling and nonparametric kernel density estimation [30] are used to quantify the uncertainty in the prediction error of PV carrying capacity, and finally confidence intervals are obtained for different conditions of PV.

Assuming U is a quantitative thesis, A is a qualitative concept in the thesis U, and x is a random number in U, and assuming that there exists a correspondence $z = f_A(x)$, which is the degree of affiliation of x corresponding to A, the distribution of x in the thesis U becomes a cloud, and the random number x is a cloud droplet which is the basic unit of the cloud model. Usually cloud models have three qualitative characteristic quantities: expectation E_x, entropy E_n, and hyperentropy H_e. where E_x is the expectation of the distribution of cloud droplets in U space. E_n is the degree of qualitative conceptual uncertainty, which is jointly determined by the degree of discretization and fuzziness. And H_e represents the uncertainty of entropy, i.e., the entropy of entropy.

The forward cloud generator belongs to the conversion process from qualitative to quantitative, i.e., the feature quantities E_x, E_n, H_e and the number of cloud droplets N are known to generate a normal random number x with E_x as the expectation, and E_n as the standard deviation, and utilize the H_e to solve the problem of the degree of affiliation of x corresponding to affiliation z of A until N cloud drops are generated.

The inverse generator, on the other hand, is a quantitative-to-qualitative transformation that solves for three eigenvalues using data x that conforms to a certain deterministic information sample. The calculations are as follows:

E_x:

$$E_x = \frac{1}{n}\sum_{i=1}^{n} x_i \tag{18}$$

E_n:

$$E_n = \sqrt{\frac{\pi}{2}} \cdot \frac{1}{n}\sum_{i=1}^{n} | x_i - E_x | \tag{19}$$

H_e:

$$\begin{aligned} H_e &= \sqrt{S^2 - {E_n}^2} \\ S^2 &= \frac{1}{n-1}\sum_{i=1}^{n}(x_i - E_x)^2 \end{aligned} \tag{20}$$

where n is the number of samples, i is the ith sample, and x_i is the difference between the predicted size and the actual size of the ith sample. s is the sample standard deviation.

Let the power prediction error be the qualitative concept A, and a be the one-time quantized representation of concept A, then $f_A(a)$ is the certainty of the one-time quantized representation of concept A, and the solution $f_A(a)$ is the process of quantized realization of the qualitative concept A, and the process of cloud droplet generation in the concept of cloud model.

In the PV carrying capacity prediction uncertainty analysis, the cloud model E_x represents the average of the power prediction error magnitude. The E_n denotes the fluctuation range of the prediction error magnitude. H_e denotes the concentration of the fluctuation range of the power prediction error magnitude.

II. C. 2) Non-parametric kernel density estimation

In this paper, when carrying out the uncertainty analysis of PV carrying capacity prediction, the cloud model is first used to qualitatively analyze the distribution of wind and PV power prediction errors, and then non-parametric kernel

density estimation and confidence intervals are used to quantitatively compute the distributional characteristics of uncertainty in the PV carrying capacity prediction.

Non-parametric kernel density estimation is different from parametric statistical methods, which does not need to make assumptions about the overall distribution of the sample in advance, and the key point is to analyze the corresponding distributional characteristics of the data directly from the sample itself, which is of wide practical value. The prediction error of photovoltaic carrying capacity is stochastic, and the fluctuation range is large with strong uncertainty, so the univariate kernel density estimation method is chosen to complete the quantitative analysis of the power prediction error.

Let the number of samples for N independent random variable $X=(X_1,X_2,X_3\ldots X_n)$, the variable random probability distribution function and the cumulative distribution function $f(x),F(x)$ relationship is as follows:

$$f(x)=F(x)^{'}=\lim_{h\to 0}\frac{F(x+h)-F(x-h)}{2h} \tag{21}$$

The empirical distribution function is one of the most commonly used estimation functions in with the following formula:

$$F_N(x)=\frac{1}{N}\sum_{i=0}^{N}X_i \quad X_i\le x \tag{22}$$

The density function for nonparametric kernel density estimation can be obtained from the above equation as:

$$\begin{aligned}\hat{f}_N(x)&=\frac{F_N(x+h)-F_N(x-h)}{2h}\\&=\frac{1}{Nh}\sum_{i=1}^{N}g(\frac{x_i-x}{h})\end{aligned} \tag{23}$$

where g is the kernel function, N is the number of interval samples, h is the bandwidth coefficient, and x_i is the i th sample.

Nonparametric kernel density estimation based on Gaussian kernel function has more advantages, for this reason, this paper adopts Gaussian kernel function as the kernel function for nonparametric kernel density estimation.

Gaussian kernel function:

$$g(x)=\frac{1}{\sqrt{2\pi}}e^{-\frac{(x-u)^2}{2\sigma}} \tag{24}$$

II. C. 3) Confidence intervals based on nonparametric kernel density estimation

After obtaining the probability density distribution of the PV carrying capacity prediction error through nonparametric kernel density estimation, the probability density distribution can be quantified using confidence intervals.

The PV carrying capacity prediction error is the difference between the predicted value P_{fore} and the actual value P_{ture} at a point in time as follows:

$$e=P_{fore}-P_{true} \tag{25}$$

For bearing capacity errors, the confidence level is calculated using the following formula:

$$P(e_{low}<e<e_{up})=1-\theta \tag{26}$$

where the interval $[e_{low},e_{up}]$ is called the confidence interval under the confidence level of $1-\theta$, e_{bw} is the lower limit of the confidence interval, and e_{up} is the upper limit of the confidence interval. $P(e_{bw}<e<e_{wp})$ denotes the probability that the bearing capacity prediction error value e falls into the interval $[e_{bw},e_{wp}]$. From this, the confidence interval for the bearing capacity prediction is $[P_{fore}-e_{low},P_{fore}+e_{up}]$.

The confidence intervals are evaluated in terms of coverage and interval width. The coverage rate δ_p describes how the confidence interval covers the real value, and the larger the coverage rate is, the more real the confidence interval can reflect the distribution of the actual value of the carrying capacity.

The formula for calculating the coverage ratio is as follows:

$$\delta_p = \frac{1}{N} \times \sum_{i=1}^{N} \partial_i \tag{27}$$

where n is the total number of samples and $\hat{c}_i$ is the coverage factor, when the actual carrying capacity falls within the confidence interval, then $\hat{c}_i = 1$, otherwise $\partial_i = 0$.

The interval width $\Delta\bar{P}$, on the other hand, is a measure of the effectiveness of the prediction, and the smaller the interval width, the better the prediction under the premise of guaranteeing the coverage. The formula for interval width is as follows:

$$\Delta\bar{P} = \frac{\sum_{i=1}^{N} \Delta P_i}{N} \tag{28}$$

where ΔP_i is the difference between the upper and lower limits of the confidence interval in which the i th power value is located.

II. D.Data preparation

Considering the multiple factors of grid topology, bus size operation mode and load level, the PV carrying capacity assessment data of the distribution network mainly comes from three sources: historical operation data, equipment labeled operation data or historical data, and real-time observed data of the distribution network.

Distribution network parameter information data are primary grid wiring diagrams and impedance parameter values. Equipment rated data are equipment rated parameters and specified equipment operating limit parameters, etc. Operational data includes data on operational parameters under normal operation of the distribution network. Distribution grid PV carrying capacity assessment needs data sources, classification and its role are listed in the above table, according to the needs of the corresponding data can be selected for distribution grid PV carrying capacity assessment.

(1) Distribution network data

Distribution network primary frame wiring diagram, distribution network equivalent impedance parameter values. Through the collection of distribution network primary frame wiring diagram and grid equivalent impedance parameters, it is clear that the scope of the carrying capacity needs to be assessed.

The busbar operation size mode and its short circuit impedance for each voltage level. Calculation of short-circuit impedance is to calculate the short-circuit capacity, short-circuit capacity can be determined by the accessible PV capacity usually does not have a priori, will be verified in the form of calibration of the PV access to meet the short-circuit capacity and short-circuit current limit requirements.

(2) Equipment rating data

The rated parameters of the distribution network equipment and the specified parameters of the equipment operating limits. The rated parameters of the distribution network equipment mainly include the voltage level applicable to the equipment and the current limit value that can be circulated under the operating condition.

(3) Operation data

Distribution network operation size mode data. The operation size data not only includes the bus size operation data but also includes the power operation data under normal operation of the distribution network. The evaluation process studied in this paper does not take into account the impact of the operation mode, so this part of the data can be used in the actual carrying capacity assessment.

Distribution network operation data. First of all, it is necessary to determine the load level of the distribution network, bus voltage, voltage, current, branch current distribution, harmonic pollution under the established load level. Using this as the base data, the PV is connected to the distribution network to assess whether the above operational data is out of bounds. It should be noted that the operational data need to be selected during normal operation, and if the operational data of the distribution network exceeds the limit values before accessing the PV, the PV carrying capacity assessment of the distribution network will not be carried out.

III. Results and analysis

III. A. Quantitative assessment of critical carrying capacity of PV in distribution networks

In this algorithm, distribution grid PV operation under different abandonment rates is used as a comparison scenario to analyze the impact of node voltage, branch currents, network losses, and PV access capacity on distribution grid operation using node voltage, branch currents, network losses, and PV access capacity as reference indicators. Quantitatively analyze the critical carrying capacity of PV in the distribution grid system under the premise of safe

and economic operation of the distribution grid. The simulation calculates ±8% system node voltage offset rate and +10% branch current maximum overload as the judgment condition of distribution grid safe operation, and the maximum system network loss as the constraint of grid economic operation. Table 1 shows the simulation comparison results under different abandonment rates.

From the results in the table, it can be seen that with the increase of PV power abandonment rate, the total load of the distribution system is increasing, and the node voltage offset, branch current overload and total system network loss also increase. If the maximum system node voltage offset and branch current overload are used as a comprehensive measure of the constraints on the actual PV acceptance capacity of the distribution network, the iterative tidal current calculation shows that the maximum PV abandonment rate that can be admitted to the PV is 3.5%. At this time, the maximum overload and maximum network loss are 6.495 MW and 0.712 MW, respectively, and the acceptable capacity of PV also stabilizes to 16.791 MW.When the number of PVs in the distribution network exceeds this scale, there will be unstable balance node voltages and branch current overload exceeding 10% of the safe operation margin under each time section. The average network loss rate of the system exceeds 5%, which seriously affects the safe and economic operation of the grid.

Table 1: Simulation comparison results of different rejection rates

Rejection rate (%)	Voltage offset	Tidal current overload rate	Maximum overload (MW)	Maximum net loss (MW)	Access capacity (MW)
0	0.371	0	/	0.124	14.315
0.5	0.394	0.03	4.188	0.192	14.322
1	0.375	0.03	4.597	0.278	15.537
1.5	0.351	0.03	4.967	0.329	15.671
2	0.397	0.06	5.082	0.407	15.958
2.5	0.358	0.06	5.588	0.532	15.959
3	0.373	0.06	6.081	0.602	16.518
3.5	0.429	0.06	6.495	0.712	16.791
4	0.572	0.09	6.943	0.808	16.842
4.5	0.606	0.09	7.629	0.914	16.917
5	0.714	0.09	8.394	1.073	16.944

III. B. Comparison of the results of PV carrying capacity assessment by different methods

In order to verify the evaluation results of the proposed method and its advantage in computational efficiency, this section evaluates the admittance capacity of the feeder and its three connected power supply stations using three different comparative methods, namely, the original Monte Carlo method (MCM), the long and short-term memory neural network (LSTM), and the convolutional neural network (CNN). The comparison results of the evaluation results of each method and its efficiency are shown in Table 2.

From the table, it can be seen that there is a slight difference between the evaluation results of the method proposed in this paper and the traditional Monte Carlo method, which are 6.73 MW and 6.71 MW, respectively. This difference mainly stems from the stochastic character of Monte Carlo simulation. In contrast, the LSTM and CNN models yielded results of 7.77 MW and 7.49 MW, respectively.This significant difference is mainly due to the fact that the two intelligent optimization algorithms treat the distribution network PV configuration scenarios as individuals in the population during the evaluation process, and thus tend to find the optimal distribution network PV configuration scheme. However, in practice, the optimal configuration does not always fully reflect the true admittance capacity of the distribution grid. Any deviation in the distribution grid PV configuration may lead to constraint violations, which in turn may affect the operational safety of the grid. In contrast, the stochastic differential equation method is able to provide more accurate assessment results by simulating a large number of configuration scenarios, which helps to ensure the safe and stable operation of the system.

In addition, as seen from the computation time comparison in the table, the computational efficiency of the proposed method in this paper is improved by 23.18% to 71.22% compared with the comparison method. The computational efficiency of the original Monte Carlo method is the lowest, which is mainly due to the fact that the original Monte Carlo method starts with no PV configuration of the system and gradually increases the capacity of the PV configuration to assess the final admittance capacity, which requires more scenarios to be computed. In contrast, the method in this paper significantly reduces the number of scenarios required in the stochastic simulation process by first performing a preliminary measurement of the admittance capacity and further evaluating it on this

basis. The method proposed in this paper proves to be effective in balancing the accuracy and timeliness of PV admittance calibration.

Table 2: The comparison results of the evaluation results and their efficiency

Models		Ours	MCM	LSTM	CNN
Check result (MW)	Feeder 1	5.44	5.38	6.21	6.13
	Platform area 1	0.62	0.65	0.74	0.66
	Platform area 2	0.41	0.43	0.53	0.49
	Platform area 3	0.26	0.25	0.29	0.21
	Total	6.73	6.71	7.77	7.49
Computation time (s)		13.26	46.07	19.13	17.26

III. C. PV Bearing Capacity Prediction Error Uncertainty Analysis

In order to verify the uncertainty of PV carrying capacity assessment based on stochastic differential equation modeling, an experiment on PV carrying capacity prediction for distribution networks is designed in this section. Ten access nodes are selected to connect distributed PV power plants to a regional power system, which together form the experimental environment. The training data in the arithmetic examples in the paper are collected in the PV power generation field nodes, and the data size in this paper is around 2.3G, and the data processing process is almost not affected by the data size.

In order to facilitate the experiment, set the PV grid-connected process, the power system lines and transformer capacity will not produce any changes, only need to consider the changes in current, voltage and power, simplify the experimental process, and facilitate the acquisition of experimental results. Based on the above experimental preparation stage, the distributed PV load-bearing capacity prediction experiments are carried out, and the PV load-bearing capacity prediction time and prediction error show the application performance of the proposed method.

Using the nonparametric kernel density estimation method, the results of the PV carrying capacity prediction confidence intervals are calculated as shown in Figure 1. From the figure, it can be seen that the PV carrying capacity prediction results obtained by applying the proposed method in this paper fall completely inside the 95%, 90%, and 85% confidence intervals, which are almost consistent with the actual results. At PV access node 3, the PV carrying capacity obtained by the proposed method is 290.90 W, and the actual result is 290.69 W, which indicates that the PV carrying capacity prediction error of the proposed method is small and the accuracy is high.

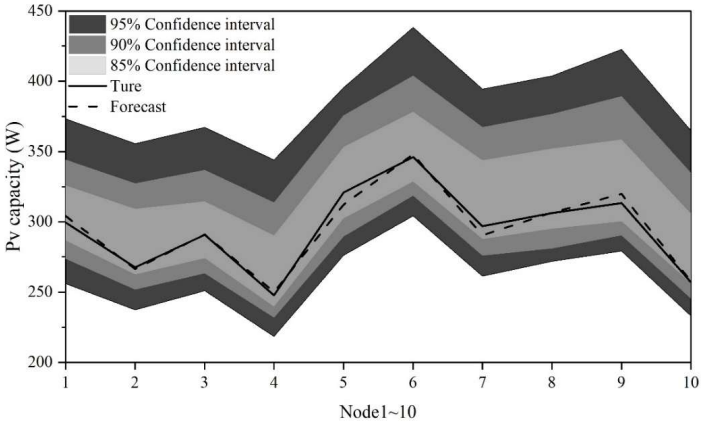

Figure 1: Pv capacity prediction interval

In order to further verify the superiority of the proposed method, the method proposed in this paper is compared with the three methods above, and the test index is the PV bearing capacity prediction error, and the results of the comparison of the prediction errors of different methods are shown in Fig. 2. It can be seen that the PV carrying capacity prediction error obtained by applying the stochastic differential equation model is 0%~3%, the PV carrying capacity prediction error of the MCM method is 3%~5%, and the prediction error of the LSTM and CNN methods is more than 8%. It shows that the prediction error of PV carrying capacity based on stochastic differential equation model in this paper is small and the accuracy is high. The above experimental results show that the PV bearing capacity prediction results obtained by the proposed method in this paper are almost consistent with the actual results, which fully confirms the better bearing capacity prediction effect of the proposed method.

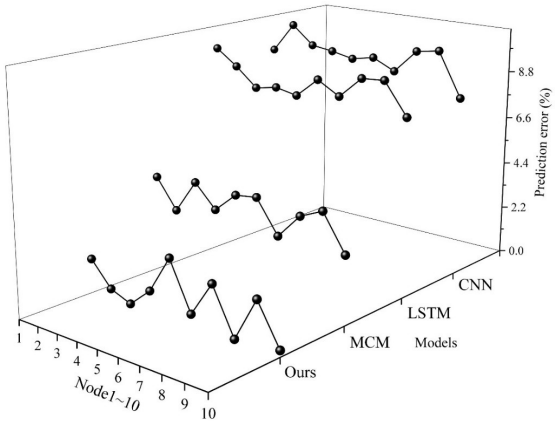

Figure 2: Comparison results of different methods of prediction error

III. D. Simulation analysis of PV carrying capacity of county distribution network

In the 10-node wiring diagram of the county distribution network in Fig. 3, residential loads are connected to nodes 2 to 10, and distributed PV is installed on the roofs of 816 households in the county area, and the area of distributed PV panels can be installed on each household is about 20 m², and each household has 10 panels, and each PV panel has the capacity of 500 Wp, and each household installs a total of 5.0 kW of PV capacity, and a total of 4080 kW of distributed PV capacity is installed in the county area. The total installed capacity of distributed PV in the county is 4080kW, and the distributed PV connected to the roofs of the residents are all generating electricity on the user side, which can be self-generated and self-consumed with the surplus power on the Internet.

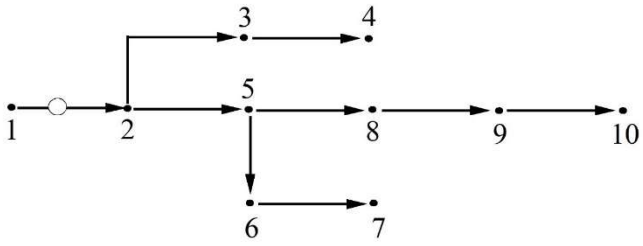

Figure 3: The county domain distribution network 10 node connection diagram

The daily output curve of distributed PV installed on the rooftop of each home in this county area is shown in Figure 4. From the figure, it can be seen that the PV begins to produce power at approximately 6:00 a.m. each day and reaches its maximum capacity of nearly 5.0 kw at approximately 12:00 p.m. Immediately afterward, the PV power level begins to decrease and stops producing power at nearly 20:00 p.m. in the evening. Since the survey was conducted during the month of July, the sun appeared at 6:00 a.m. in the county and the PV began generating power. It was not until 20:00 p.m. when the sun completely set and power generation ceased.

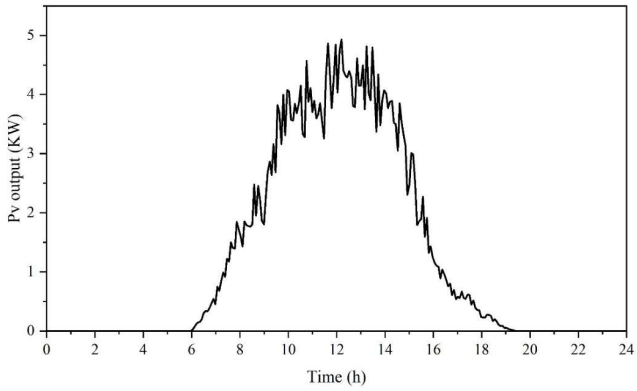

Figure 4: PV daily output curve

The county is categorized into three types based on the electricity usage of different residents in the county. The daily load profiles of the three residential types are shown in Figure 5, with the black dash line representing the residential daily load profiles at nodes 2, 3, and 4, the black dashed line representing the residential daily load profiles at nodes 5, 6, and 7, and the gray dash line representing the residential daily load profiles at nodes 8, 9, and 10.

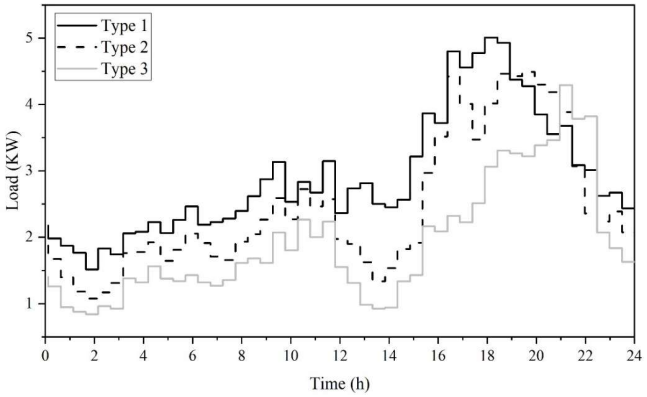

Figure 5: Daily load curve of residents

In order to obtain the maximum PV carrying capacity in the county distribution network, the distributed PV grid-connected model under different acceptance rates is subjected to current simulation calculations to analyze the impact of distributed PV under different acceptance rates on the sensitive point voltage, and the maximum PV acceptance rate and carrying capacity of the county distribution network at this time are sought when the sensitive point voltage is satisfied as the upper limit value (1.07 pu). Figure 6 demonstrates the value of the sensitivity point voltage under different PV admittance rates.

The simulation results show that with the increase of distributed PV acceptance rate, the value of the sensitive point voltage gradually increases, and when the acceptance rate is 1, the sensitive point voltage is 1.088 pu, at this time, the sensitive point voltage has crossed the limit of 0.018 pu. When the value of the voltage at the sensitive point is 1.07 pu, the voltage at the sensitive point at this time just reaches the upper voltage limit, which corresponds to the distributed PV admittance rate of 0.65, indicating that when the distributed PV admittance rate is 0.65 for the maximum PV admittance rate of the distribution network in the county. The PV admittance rate k is the ratio of PV output to PV capacity, i.e.:

$$k = \frac{P_{out}}{P_N} \tag{29}$$

Since the total installed distributed PV capacity in this county area is 4080kW, from the above equation, the maximum distributed PV output in this county area is 2652kW, i.e. the maximum PV carrying capacity in this county area is 2652kW.

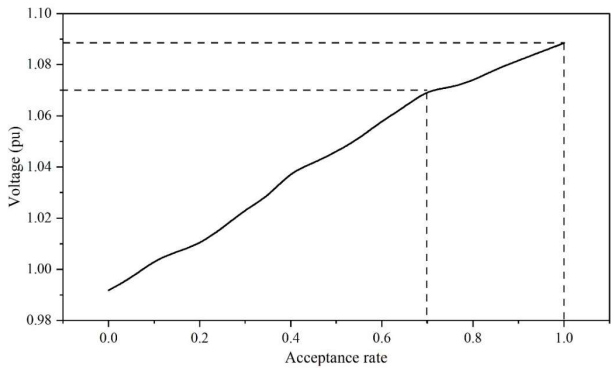

Figure 6: Sensitive point voltage value of different photovoltaic acceptance rate

IV. Conclusion

The study builds a one-dimensional stochastic differential equation model for the assessment of PV carrying capacity of county distribution grids, and uses this model to solve for the maximum PV capacity under different constraints. Inputting the distribution system topology and line parameters as well as the set PV capacity, a stochastic utilization scenario is generated, and the stochastic differential equations are used to calculate the PV output profile. Based on this, the PV treatment curve is summed up to calculate the final abandonment rate. When the resulting discard rate reaches the set conditions, the maximum PV access capacity can be obtained. At the same time, the univariate kernel density estimation method is used to quantify the PV carrying capacity prediction uncertainty distribution.

(1) When the PV light abandonment rate exceeds 3.5%, the branch current overload of the distribution network exceeds 10%, and the average network loss rate exceeds 5%, which affects normal operation.

(2) The PV carrying capacity assessment result of the power supply station area under the stochastic differential equation model is 6.73 MW, which is accurate and the calculation time is improved by 23.18% to 71.22% compared with the comparison method.

(3) The prediction error of PV carrying capacity of this paper's method is between 0% and 3%, which is much lower than the comparison method.

(4) The method of this paper predicts that the maximum PV capacity, i.e. 2652kW, is reached when the distributed PV acceptance rate of a county is 0.65.

References

[1] Luo, N., Lu, Z., Liu, J., Zhang, P., Chen, L., He, H., ... & Zhang, Y. (2024, September). Research on Evaluation Index System of County Distribution Network Planning under New Power System. In 2024 The 9th International Conference on Power and Renewable Energy (ICPRE) (pp. 506-511). IEEE.

[2] LI, M., LIU, W., LI, P., TIAN, C., GAO, Y., ZHANG, B., ... & HU, P. (2021). Method for allocation of county distribution network considering the investment benefit evaluation. Journal of Electric Power Science and Technology, 35(6), 83-89.

[3] Yang, L., Peng, D., Liu, H., Cheng, Y., & Guo, N. (2022, July). Collaborative optimization of wind-solar-storage configuration in county distribution network considering near-zero carbon emission. In 2022 IEEE/IAS Industrial and Commercial Power System Asia (I&CPS Asia) (pp. 1283-1291). IEEE.

[4] Zhang, J., Xiong, L., Yuan, J., Duan, X., & Wu, B. (2014). The research on how to improve the reliability of county-level distribution grids using the TD-LTE process. In Engineering Technology and Applications (pp. 259-266). CRC Press.

[5] Yi-yang, L. U. O. (2022). How to Improve the Distribution Network Operation and Maintenance Level of County-level Power Supply Company. Rural Electrification, (9), 92-93.

[6] TAN, X., HU, S., ZHANG, J., ZHOU, X., HE, C., & SU, J. (2022). Investment benefit assessment based on PCA and weighted TOPSIS in county distribution network. Journal of Electric Power Science and Technology, 37(3), 133-139.

[7] Ritzen, M. J., Houben, J. J. M., Rovers, R., Vroon, Z. A. E. P., & Geurts, C. P. W. (2019). Carrying capacity based environmental impact assessment of Building Integrated Photovoltaics. Sustainable Energy Technologies and Assessments, 31, 212-220.

[8] Xia, X., Wang, X., Zhang, H., Xu, F., Ye, S., Liu, H., & Li, Q. (2023). Assessment of the carrying capacity of distributed generation in distribution network considering soft open point. Energy Reports, 9, 151-159.

[9] Ayaz, M. S., Malekpour, M., Azizipanah-Abarghooee, R., Karimi, M., & Terzija, V. (2024). Probabilistic photovoltaic generation and load demand uncertainties modelling for active distribution networks hosting capacity calculations. International Journal of Electrical Power & Energy Systems, 159, 110016.

[10] Mansouri, N., Lashab, A., Guerrero, J. M., & Cherif, A. (2020). Photovoltaic power plants in electrical distribution networks: a review on their impact and solutions. IET Renewable Power Generation, 14(12), 2114-2125.

[11] Chai, Y., Guo, L., Wang, C., Zhao, Z., Du, X., & Pan, J. (2018). Network partition and voltage coordination control for distribution networks with high penetration of distributed PV units. IEEE Transactions on Power Systems, 33(3), 3396-3407.

[12] Wang, L., Yuan, M., Zhang, F., Wang, X., Dai, L., & Zhao, F. (2019). Risk assessment of distribution networks integrating large-scale distributed photovoltaics. IEEE access, 7, 59653-59664.

[13] Bendík, J., Cenký, M., Cintula, B., Beláň, A., Eleschová, Ž., & Janiga, P. (2022). Stochastic approach for increasing the PV hosting capacity of a low-voltage distribution network. Processes, 11(1), 9.

[14] Zhang, H., Tong, X., & Yin, J. (2019). Influence of distributed photovoltaic power generation on distribution network and the design of optimal access scheme. The Journal of Engineering, 2019(16), 1361-1367.

[15] Chen, S., Zhang, Y., & Zheng, J. (2021). Assessment on global urban photovoltaic carrying capacity and adjustment of photovoltaic spatial planning. Sustainability, 13(6), 3149.

[16] Zhang, L., Lei, Z., Ye, Z., & Peng, Z. (2024). Distributed PV carrying capacity prediction and assessment for differentiated scenarios based on CNN-GRU deep learning. Frontiers in Energy Research, 12, 1481867.

[17] Yan, G., Wang, Q., Zhang, H., Wang, L., Wang, L., & Liao, C. (2024). Review on the Evaluation and Improvement Measures of the Carrying Capacity of Distributed Power Supply and Electric Vehicles Connected to the Grid. Energies, 17(17), 4407.

[18] Torquato, R., Salles, D., Pereira, C. O., Meira, P. C. M., & Freitas, W. (2018). A comprehensive assessment of PV hosting capacity on low-voltage distribution systems. IEEE Transactions on Power Delivery, 33(2), 1002-1012.

[19] Yao, H., Qin, W., Jing, X., Zhu, Z., Wang, K., Han, X., & Wang, P. (2022). Possibilistic evaluation of photovoltaic hosting capacity on distribution networks under uncertain environment. Applied Energy, 324, 119681.

[20] Zhao, Z., Li, Y., Sun, Q., Li, R., Ma, Z., & Guo, D. (2024). Assessment of the Distributed Generation Carrying Capacity in New-Type Distribution Networks Based on Different Load Levels. Distributed Generation & Alternative Energy Journal, 1069-1096.

[21] Mulenga, E., Bollen, M. H., & Etherden, N. (2021). Solar PV stochastic hosting capacity in distribution networks considering aleatory and epistemic uncertainties. International Journal of Electrical Power & Energy Systems, 130, 106928.
[22] Chen, C., Peng, W., Xie, C., Dong, S., & Hua, Y. (2025). Photovoltaic Hosting Capacity Assessment of Distribution Networks Considering Source–Load Uncertainty. Energies, 18(8), 2134.
[23] Fatima, S., Püvi, V., & Lehtonen, M. (2020). Review on the PV hosting capacity in distribution networks. Energies, 13(18), 4756.
[24] Meng, L., Yang, X., Zhu, J., Wang, X., & Meng, X. (2024). Network partition and distributed voltage coordination control strategy of active distribution network system considering photovoltaic uncertainty. Applied Energy, 362, 122846.
[25] Wang, S., Dong, Y., Wu, L., & Yan, B. (2019). Interval overvoltage risk based PV hosting capacity evaluation considering PV and load uncertainties. IEEE transactions on smart grid, 11(3), 2709-2721.
[26] Fan, G. F., Feng, Y. W., Peng, L. L., Huang, H. P., & Hong, W. C. (2024). Uncertainty analysis of photovoltaic power generation system and intelligent coupling prediction. Renewable Energy, 234, 121174.
[27] Connor Delaosa,Jennifer Pestana,Ian K. Proudler & Stephan Weiss. (2025). Impact of space–time covariance matrix estimation on bin-wise eigenvalue and eigenspace perturbations. Signal Processing,233,109946-109946.
[28] Subramanian Ramakrishnan & Aman Kumar Singh. (2024). Stochastic dynamics of a nonlinear vibration energy harvester subjected to a combined parametric and external random excitation: The distinct cases of Itô and Stratonovich stochastic integration. International Journal of Non-Linear Mechanics,162,104700-.
[29] Kuznetsov Dmitriy Feliksovich. (2023). Mean-square Approximation of Iterated Ito and Stratonovich Stochastic Integrals: Method of Generalized Multiple Fourier Series. Application to Numerical Integration of Ito Sdes and Semilinear Spdes (third Edition). Differential Equations and Control Processes,(1),151-1097.
[30] Feng Renhai,Wajid Khan,Afshan Tariq,Muhammad Abbas,Muhammad Zain Yousaf,Abdul Aziz... & Milkias Tuka. (2025). Adaptive non-parametric kernel density estimation for under-frequency load shedding with electric vehicles and renewable power uncertainty. Scientific Reports,15(1),11499-11499.